

Original Article

Design and Validation of a Compact 3.5GHz Antenna for 5G-based IoT Applications

Najib Al-Fadhali^{1*}, Huda Majid¹, Jumadi¹, Mohammed. S. M. Gismalla²

¹Faculty of Engineering Technology, Department of Electrical Engineering Technology, Universiti Tun Hussein Onn Malaysia (UTHM), Malaysia.

²Center for Communication Systems and Sensing, King Fahd University of Petroleum and Minerals (KFUPM), Dhahran, Saudi Arabia.

*Corresponding Author : eng.najeebfadhali@gmail.com

Received: 03 May 2023

Revised: 20 June 2023

Accepted: 16 August 2023

Published: 03 September 2023

Abstract - Compact and small-sized antennas are crucial for 5G-based IoT applications due to their ease of integration into devices with limited space, lower power consumption, and ease of installation in urban areas. In this research, we designed a compact wideband 3.5GHz antenna for 5G-based IoT applications using CST Studio software. The antenna was fabricated on an FR-4 substrate with dimensions of 40mmx32mm and a thickness of 1.6mm, with a microstrip feeding line. Simulation results showed a return loss of -42.287dB and a VSWR of 1.016. Real measurements of S11, radiation pattern, and gain were conducted to validate the simulation results, with S11 measurements taken using a Vector Network Analyzer at the UTHM Pagoh RF Lab and radiation pattern and gain measured in a chamber at the UTeM RF Lab. The simulation and real measurement results were similar, with slight differences due to device inaccuracies and manufacturing. The designed antenna is believed to be beneficial for fifth-generation communication-based IoT applications.

Keywords - Compact 3.5GHz antenna, 5G-based IoT applications, Internet of Things.

1. Introduction

The Fifth generation of mobile networks, or 5G, is the latest and most advanced wireless communication technology that promises to revolutionize our lives, works, and communications. With its high-speed data transmission, low latency, and large network capacity, 5G has the potential to transform industries and change the way we interact with technology [1]. One of the key areas that 5G is expected to impact significantly is the Internet of Things (IoT). IoT refers to the growing network of connected devices, sensors, and machines that are able to communicate and share data with each other without human intervention. This technology can potentially revolutionize a wide range of industries, from healthcare and transportation to manufacturing and agriculture [2].

The combination of 5G and IoT technology is expected to create new opportunities for innovation and growth. 5G's high-speed data transmission and low latency will enable IoT devices to communicate with each other and the cloud in real-time, enabling new use cases and applications that were not previously possible. This will lead to the creation of smart cities, where all devices and systems are connected and able to communicate with each other, improving efficiency, reducing costs, and improving the quality of life for citizens.

Additionally, 5G will enable deploying new and advanced IoT technologies such as autonomous vehicles, smart factories, and virtual and augmented reality. However, implementing 5G-based IoT systems is not without challenges [3-5]. One of the major challenges is the design and development of compact and small-size antennas that can support the high-speed data transmission and low latency required by 5G [6]. Additionally, the increasing number of connected devices and the large amount of data they generate will also require the development of efficient and secure networks and data management systems. Overall, 5G and IoT technology are expected to impact society and industry significantly.

The deployment of 5G networks and the integration of IoT technology will enable new use cases and applications, improve efficiency, reduce costs, and improve the quality of life for citizens. However, it is important that these technologies are developed and implemented responsibly and sustainably. 5G of mobile networks is set to revolutionize how we live and work by providing faster internet speeds, lower latency, and more reliable connections [7]. The 5G technology can potentially enable a wide range of new applications and services, including IoT. IoT is a network of connected devices and sensors that collect and share data, enabling new use cases



such as remote monitoring, predictive maintenance, and smart cities. One of the major challenges in implementing 5G-based IoT systems is the design and development of compact and smart antennas. Antennas play a critical role in wireless communication systems as they are responsible for transmitting and receiving signals. In IoT applications, the compactness and small size of the antenna are crucial, as they allow for easy integration into devices with limited space, such as smartwatches, fitness trackers, and other wearable devices. In addition, compact antennas are essential for deploying IoT networks in urban areas where space is limited. The 5G frequency range is higher than previous generations, so the antennas used in 5G-based IoT systems must also be designed to operate at these higher frequencies [8].

This requires using advanced materials and techniques to achieve the necessary performance levels. In addition, IoT devices often have very limited power resources, so the antenna must be designed to be very energy efficient. Furthermore, with the increasing number of connected devices, the demand for smarter and more adaptable antennas is also increasing. Smart antennas can adapt to their environment, change their radiation pattern, and optimize their performance based on the specific needs of the device and the network. This allows the system to operate more efficiently and effectively and to support a wide range of different applications and services. In conclusion, designing and validating compact and smart antennas for 5G-based IoT applications is of great importance to ensure IoT systems' efficient and effective functioning. It is a challenging task that requires a combination of advanced materials, techniques, and smart algorithms to achieve the necessary performance levels [7]. The success of 5G-based IoT systems will depend on these antennas' availability and ability to support the diverse range of IoT applications and services. IoT is a rapidly growing technology that connects various devices and sensors to the internet, allowing for data collection and sharing in real-time. With the increasing demand for high-speed data transmission and connectivity in IoT applications, 5G technology is being developed to meet these needs.

However, one of the major challenges in implementing 5G-based IoT systems is the design and development of compact and small-size antennas that can operate in the 3.5GHz frequency band. The compactness and small size of the antenna are crucial in IoT applications, as they allow for easy integration into devices with limited space, such as smartwatches, fitness trackers, and other wearable devices [2]. In addition, compact antennas are essential for deploying IoT networks in urban areas where space is limited. A compact antenna that operates in the 3.5GHz frequency band and is wide band can cover a large area and a lot of sensors [9]. This allows for higher data transmission rates, lower power consumption, and ease of installation. The design and

validation of a compact wideband 3.5GHz antenna for 5G-based IoT applications are of great importance to ensure IoT systems' efficient and effective functioning. A compact antenna that can cover a wide frequency range and operate in multiple directions will be able to handle a large number of sensors and devices and provide high-speed data transmission. This is becoming increasingly important as IoT technology continues to expand and more devices are connected to the internet [10].

This paper aims to address the challenges of designing and developing compact and small-size antennas that can operate on 3.5GHz wide band frequencies for 5G-based IoT applications. The increasing demand for high-speed data transmission and connectivity in IoT systems has led to the development of 5G communications (5G) technology. However, one of the major challenges in implementing 5G-based IoT systems is the design and development of compact and small-size antennas that can cover a wide area and support multiple sensors. The compactness and small size of the antenna are crucial in IoT applications, as they allow for easy integration into devices with limited space, such as smartwatches, fitness trackers, and other wearable devices. In addition, compact antennas are essential for deploying IoT networks in urban areas where space is limited. The small size also allows for lower power consumption and ease of installation. Therefore, the design and validation of compact 3.5GHz antennas for 5G-based IoT applications is of great importance to ensure IoT systems' efficient and effective functioning. This paper aims to design, fabricate and validate a compact, smart, multi-directional 3.5GHz wideband antenna for IoT applications with 5G frequency.

2. Literature Review

The advancement of IoT has led to an increasing demand for high-speed data transmission and connectivity, which has, in turn, driven the development of 5G technology. However, the implementation of 5G-based IoT systems poses a number of challenges, one of which is the design and development of compact and small-size antennas. The compactness and small size of the antenna are crucial in IoT applications, as they allow for easy integration into devices with limited space, such as smartwatches, fitness trackers, and other wearable devices. In addition, compact antennas are essential for deploying IoT networks in urban areas where space is limited. The small size also allows for lower power consumption and ease of installation. In order to address these challenges, many researchers have focused on developing compact and efficient antennas for 5G-based IoT applications [11]. One of the key areas of research has been the use of microstrip antenna technology, which allows for the design of small and lightweight antennas with a simple and low-cost fabrication process [12].

Additionally, researchers have also investigated the use of advanced electromagnetic simulation tools, such as the CST Studio software, to optimize the design of the [13, 14]. Several studies have also focused on the design and validation of compact antennas operating in the 3.5GHz frequency band. This frequency band is considered a suitable choice for IoT applications due to its wide bandwidth and good penetration capability. However, designing a compact 3.5GHz antenna for 5G-based IoT applications is still challenging, as it requires a balance between the antenna size and its radiation performance. It is worth noting that it is important for the antenna to have a wide band and multi-directional radiation pattern to cover a large area and many sensors, which is the main target of this research. In summary, the design and validation of a compact 3.5GHz antenna for 5G-based IoT applications is a critical research area, as it addresses the challenge of providing efficient and effective connectivity for IoT systems while also taking into account the limitations of size, power consumption, and ease of installation. This paper aims to address these challenges by presenting a design and validation of a compact 3.5GHz antenna for 5G-based IoT applications.

3. Methodology

The methodology for this research involved several steps, including the design of the antenna using CST Studio software, fabrication of the prototype, and validation through measurements. First, designing the compact 3.5GHz wideband antenna for 5G-based IoT applications was carried out using CST Studio software. The antenna design utilized an FR-4 substrate and a microstrip feeding line as the transmission line. The dimensions of the FR-4 used were 40mmx32mm with a thickness of 1.6mm. Next, the fabricated prototype was measured using a Vector Network Analyzer (VNA) to validate the simulation results. The VNA was connected to the microstrip feeding line by a subminiaturized version of a connector. The S11 measurements were conducted in the UTHM Pagoh RF Lab, while the radiation pattern and gain were measured in the UTeM RF Lab using a chamber. It is worth noting that the simulation results and real measurements were compared, with slight differences due to the inaccuracy of the devices and manufacturing.

The methodology aimed to provide a comprehensive design, fabrication and validation process of the compact wideband 3.5GHz antenna for 5G-based IoT applications. The flow chart for the project is shown in Figure 1. It consists of 4 stages. In stage 1, research on microstrip patch antenna for 5G application was conducted, and design ideas were gathered. In stage 2, the antenna was designed and simulated using Computer Simulation Technology (CST) software. If the results were satisfactory, the antenna was fabricated in the PCB lab during stage 3. If not, the design was modified, and the process was repeated until satisfactory results were obtained. In stage 4, the antenna was tested, results were

compared with the CST simulation, and findings, conclusions, and recommendations were discussed. The use of Computer Simulation Technology (CST) software is crucial in designing a 3.5 GHz antenna as it allows for virtual testing and optimization of the antenna before it is physically fabricated. This enables engineers to identify and correct any design flaws or issues before committing to the time and cost of fabrication.

Additionally, the CST software provides a detailed simulation of the antenna's performance and behavior, including its S-parameters, far-field radiation pattern, and other important metrics [13-15]. The use of FR-4 substrate material also offers several benefits in the design of a 3.5 GHz antenna. Firstly, FR-4 is a low-cost material that widely replaces flammable PCB materials. Secondly, it has a fire-resistant property, making it a safer option for PCB applications. Finally, the dielectric constant of FR-4 has a reported range between 4.3 and 4.8, making it suitable for frequencies up to 1 GHz. The loss tangent value of 0.018 also ensures low signal loss. These properties make FR-4 a suitable choice for the design of 3.5 GHz antennas, and its use can result in a cost-effective and safe solution for high-frequency circuit design.

3.1 Antenna Configuration

The calculation for the width and length of the rectangular patch to design the antenna in CST software is as follows. The speed of light in free space, c is equal to 3×10^8 m/s, ϵ_r is the dielectric constant of the substrate, f_r is the design antenna frequency, W is the width, ϵ_{eff} is the effective dielectric constant, and the dimension of the patch along a distance is ΔL as shown in equations (1) to (3)

$$W = \frac{c}{2f_r} \sqrt{\frac{2}{\epsilon_r + 1}} \tag{1}$$

$$\epsilon_{eff} = \frac{\epsilon_r + 1}{2} + \frac{\epsilon_r - 1}{2} \left(1 + \frac{12h}{W}\right)^{-1/2} \tag{2}$$

$$\frac{\Delta L}{h} = 0.412 \frac{(\epsilon_{eff} + 0.3) \left(\frac{W}{h} + 0.264\right)}{(\epsilon_{eff} + 0.258) \left(\frac{W}{h} + 0.8\right)} \tag{3}$$

The actual length of the patch can be calculated in equation (4), and the length and width of the microstrip patch ground plane can be calculated in equations (5) and (6)

$$L = \frac{c}{2f_r} - 2\Delta L \tag{4}$$

$$L_g = 6h + L \tag{5}$$

$$W_g = 6h + W \tag{6}$$

Table 1 presents the dimension of the microstrip patch calculated by the equation above.

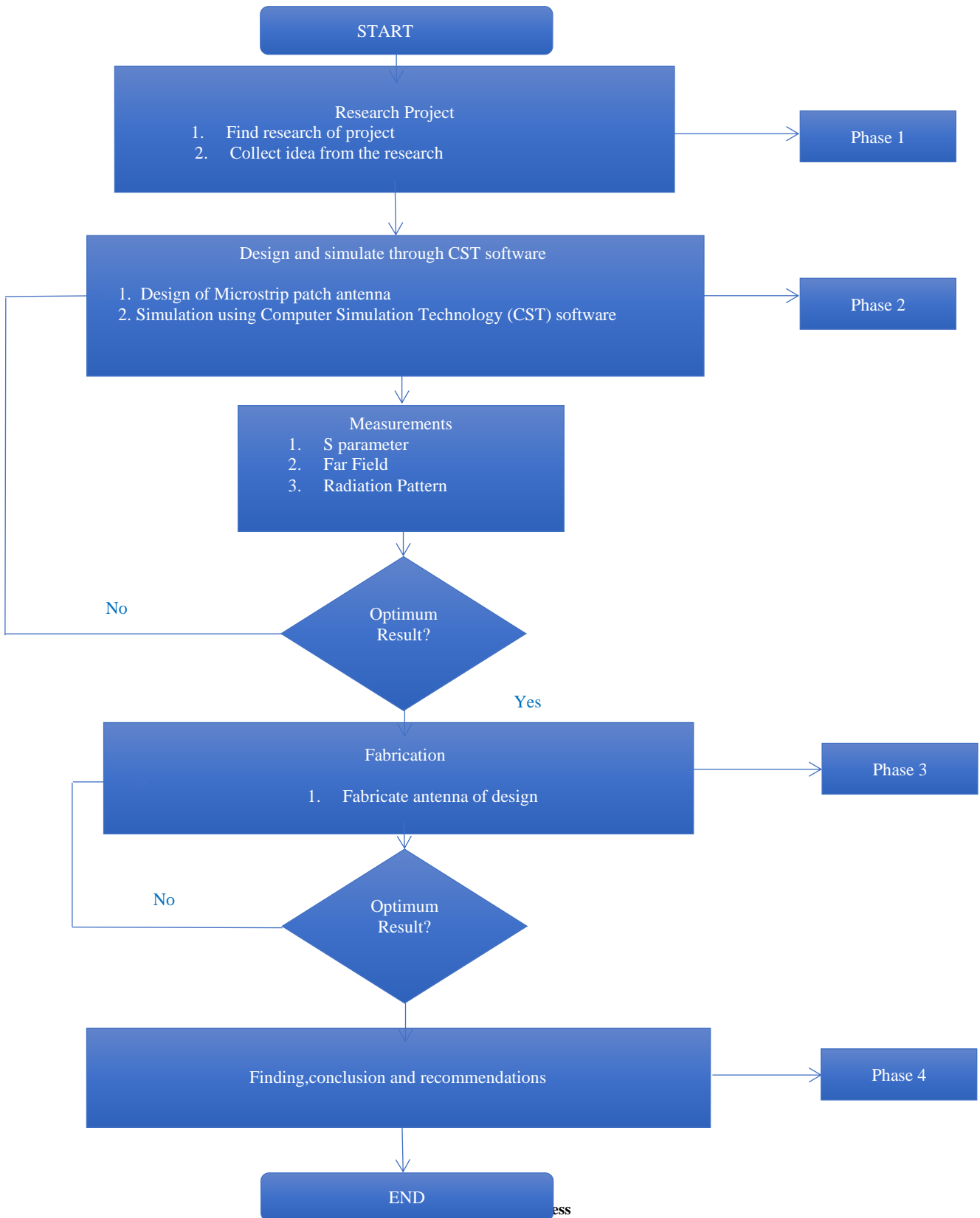


Table 1. Calculated dimension of microstrip patch by equations

Parameter	Dimension	Description
W_p	52.6539	Width of the patch
L_p	40.4330	Length of the patch
W_g	56.2538	Width of the ground plane
L_g	44.0332	Length of the ground plane

3.2. Antenna Design Specification

Microstrip patch antenna has two important design parameters

- Relative dielectric constant of the substrate (ϵ_r): The dielectric material selected for this project is FR-4, which has a relative dielectric constant 4.3.
- Height of dielectric substrate (h): The height of the dielectric substrate is selected as 1.60mm, which is the substrate thickness available in the laboratory
- Height of radiating element: The height of the radiating element is selected as 0.3mm, which is the element thickness available in the laboratory.

Table 2 provides the dimensions and properties of FR-4, a popular dielectric material used in constructing Printed Circuit Boards (PCBs) and microstrip patch antennas.

Table 2. FR-4 dimensions and properties

FR-4 parameter	Values
Dielectric constant (ϵ_r)	4.3
Substrate height (mm)	1.6
Relative permeability, (μ)	1
Dimension, (mm)	40x40

3.3. Simulation and Parametric Study

In this particular section, the antenna substrate used is the dielectric material FR-4, whose properties and dimensions are listed in Table 1. A copper patch is applied on the top surface of the FR-4 substrate, while the ground plane of the antenna is

partially covered with copper. The patch antenna is designed with a partial ground plane of a different shape, and some slots are introduced on the patch. The patch is fed using a 50-ohm microstrip line, as illustrated in Figure 2, which depicts the proposed patch antenna and ground plane. Additionally, the resonant frequency for the patch antenna is fixed at 3.5GHz and is shown in Figure 3.

Based on the dimensions and properties listed in Table 1 and Table 2, several steps are involved in designing the proposed antenna, outlined below. Firstly, a FR-4 substrate is created according to the dimensions specified in Table 2. A partially covered ground plane, with dimensions of 56.2538x44.0332x0.035mm, is then constructed on the back of the substrate.

A copper patch is also created on the front surface of the substrate with dimensions of 52.6539x40.4330x0.035mm. Additionally, a microstrip feeding line with dimensions of 3x24x0.035mm is created to connect the port with the bottom faces for measuring values. The proposed patch antenna and ground plane are illustrated in Figure 2. To evaluate the performance of the proposed design, it is simulated using CST software, and the results are presented in the following section.

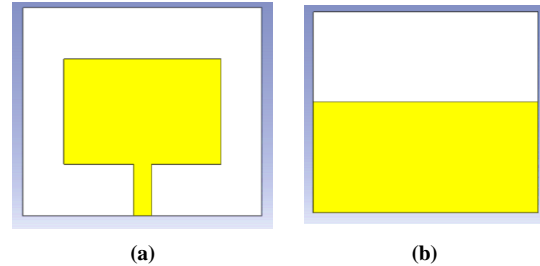


Fig. 2 (a) Proposed patch antenna, (b) Proposed ground plane

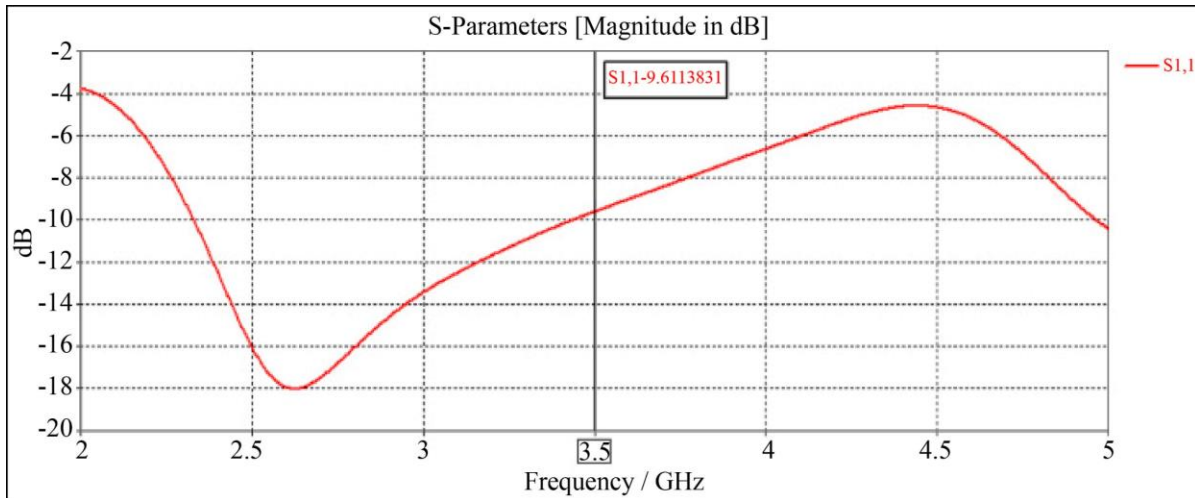


Fig. 3 S11 parameter of proposed antenna design

The results obtained from the initial design, as depicted in Figure 1, were found to be unsatisfactory. The frequency did not meet the desired target of 3.5GHz, and the return loss was around -18dB, which was unacceptable. Consequently, a parametric study was conducted to improve the antenna design. The modifications included adding slots to the patch antenna and reducing the dimensions of the ground plane. These adjustments resulted in a more compact antenna design with an increased resonant frequency, which achieved the objective of this project. The modified antenna design is presented in Figure 4, which illustrates the modification process involving the addition of slots to the patch antenna and the reduction of the ground plane dimensions.

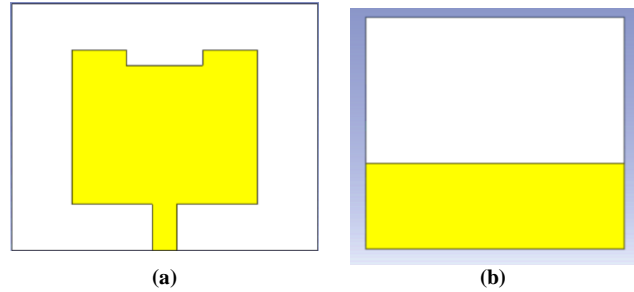


Fig. 4 Modify process (a) Add a slot on the patch, (b) Decrease the dimension of the ground plane

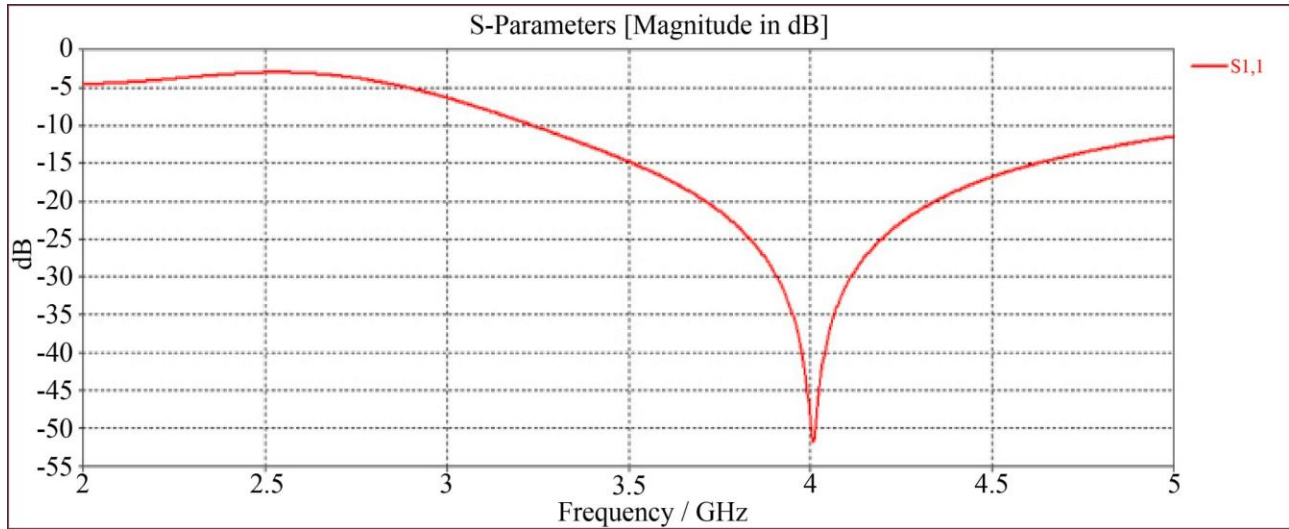


Fig. 5 S11 parameter

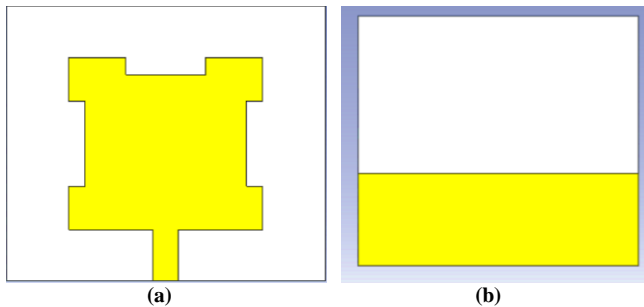


Fig. 6 Modify process (a) Add two slots on the patch, (b) Keep the dimension of the ground plane

The modification process of the antenna design, which involved the addition of slots to the patch and changes in the dimensions of the patch and ground plane, is illustrated in Figure 4 and Figure 5.

The modifications made to the antenna design, as illustrated in Figure 5, resulted in an increase in frequency to

4GHz, an improvement in return loss to around -51dB, and a wider bandwidth. However, the antenna still did not meet the objective of operating at 3.5GHz.

Consequently, further modifications were implemented to improve the antenna's output, as shown in Figure 6. The results of these modifications are presented in Figure 7, but they did not meet the requirements for the antenna to radiate at exactly 3.5GHz. The modifications included adding two slots to the patch and keeping the dimensions of the ground plane unchanged.

Figure 8 illustrates the addition of two slots to the patch antenna while keeping the ground plane dimensions unchanged. The results of this modification, as shown in Figure 9, included an increase in frequency, a decrease in return loss, and a wide bandwidth. However, the frequency still did not meet the desired objective. Therefore, the modification process was continued to improve the antenna's output.

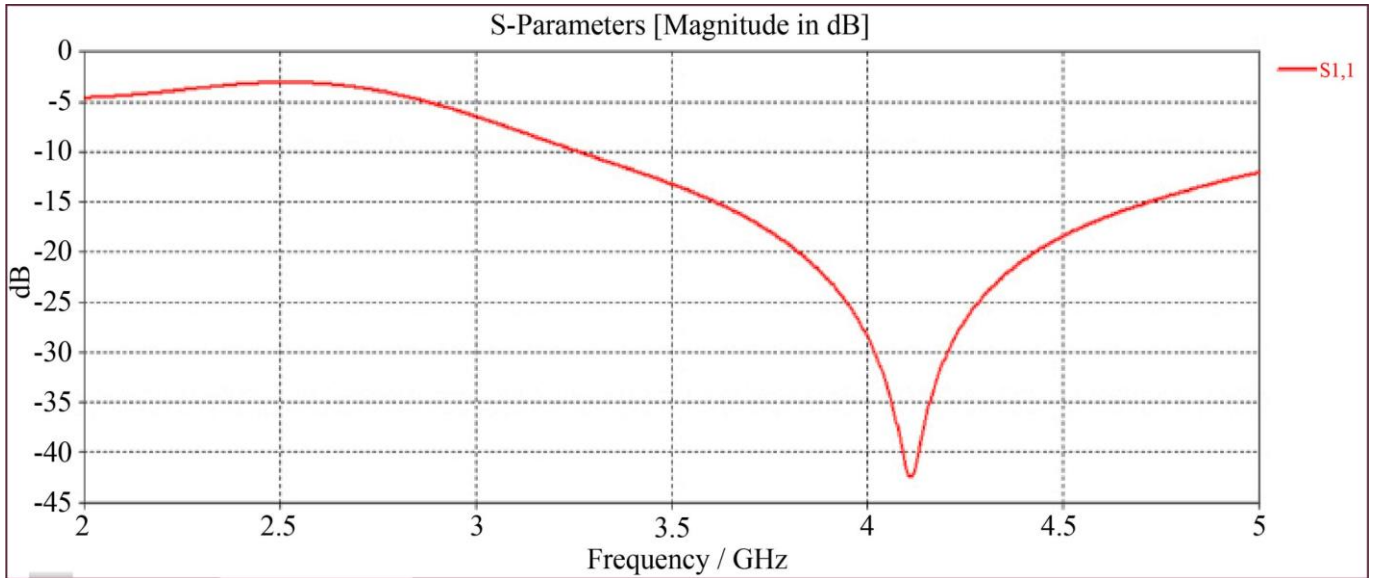


Fig. 7 S11 parameter

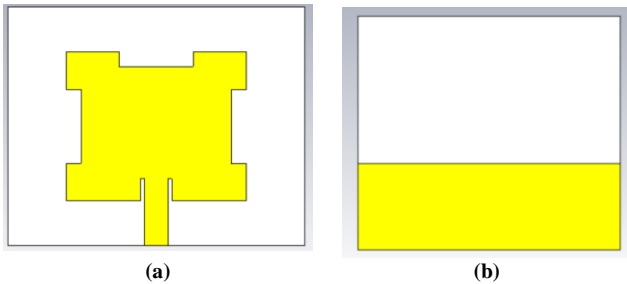


Fig. 8 Modify process (a) Add two slots on fed, (b) Keep the dimension of the ground plane

The modification process involved adding slots to the feed, as illustrated in Figure 8(a) while keeping the dimensions of the ground plane unchanged.

The results of this modification, shown in Figure 9, included a shift in frequency from 4.13GHz closer to 3.5GHz and a decrease in return loss. Although the frequency was closer to meeting the desired objective, small adjustments were still required to improve the antenna's performance further.

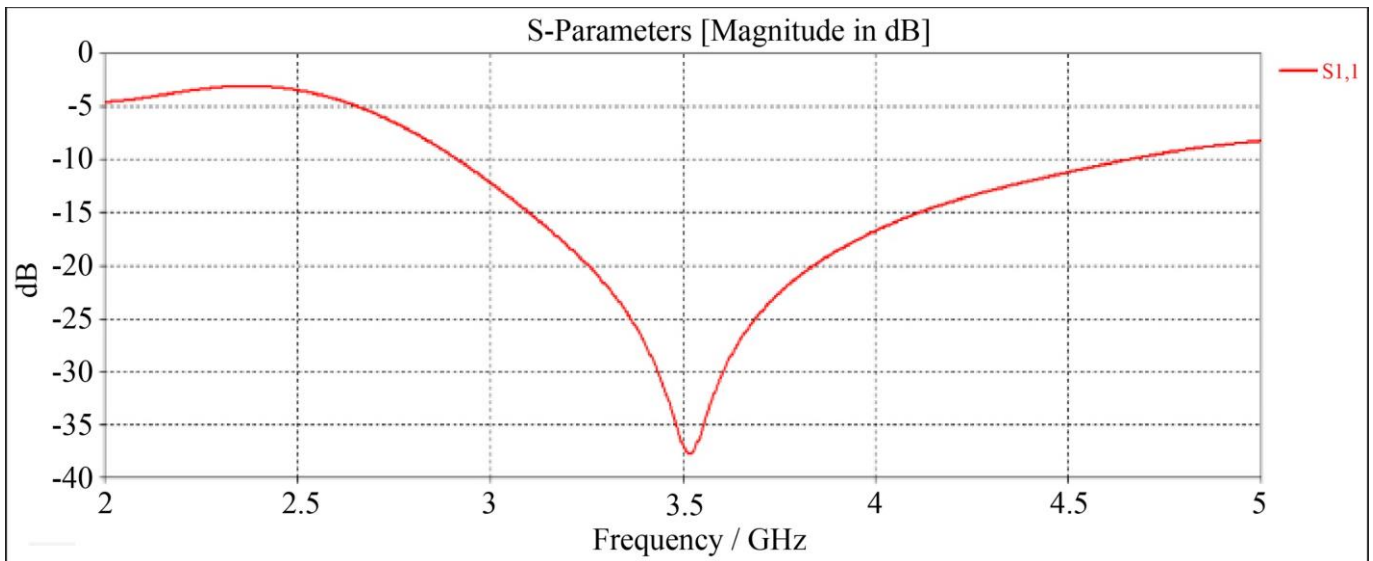


Fig. 9 S11 parameter

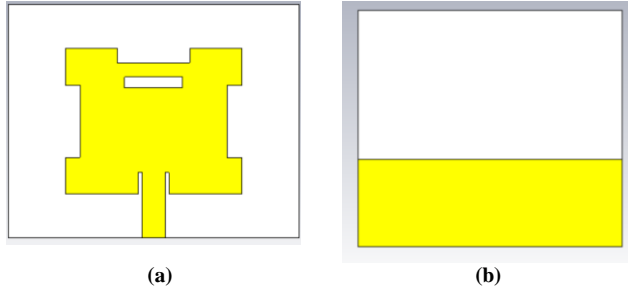


Fig. 10 Modify process (a) Add one slot on patch, (b) Keep dimension of ground

Hence, in Figure 10, one slot was added to the patch antenna and the dimensions of the ground plane were kept unchanged. Subsequently, modifications and adjustments were carried out to improve the frequency to 3.5GHz, as depicted in Figure 11. The results of these modifications show that the frequency finally meets the desired value of 3.5GHz, and the return loss is satisfactory, while the bandwidth remains wide. All the parameters and dimensions of the modified antenna are listed in Table 3. Notable changes include the dimensions of the FR-4 substrate, ground plane, patch antenna, and feed line.

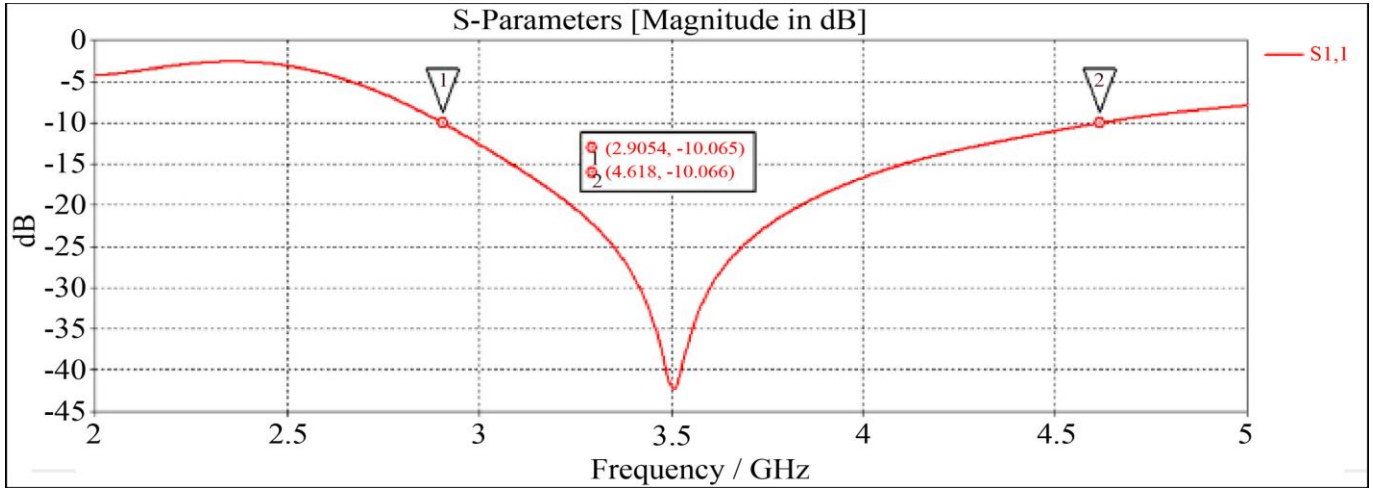


Fig. 11 S11 parameter

Table 3. Parameter and dimension of the modified antenna

Parameter	Dimension	Description
w	40	Width of FR-4 substrate
l	32	Length of FR-4 substrate
h	1.6	Height of FR-4 substrate
gw	40	Width of ground
gl	24	Length of ground
gh	0.035	Height of ground
pw	24	Width of patch
pl	20.3	Length of patch
ph	0.035	Height of patch
fw	3.2	Width of the feed line
fl	24	Length of feed line
fh	0.035	Height of feed line
sw	5	Width of the first slot
sl	4	Length of the first slot
sw2	4	Width of the second slot
sl2	5	Length of second slot
sw3	0.5	Width of the third slot
sl3	3	Length of third slot
sw4	8	Width of the fourth slot
sl4	1.5	Length of fourth slot

3.4. Fabrication Process

Validation of the simulation results of the antenna design can be achieved through fabrication. The designed antenna will be fabricated to validate the simulation results, and the Vector Network Analyzer (VNA) will be used to measure the results. The antenna can be fabricated using the steps illustrated in Figure 12.

The design, consisting of a patch antenna and a ground plane, is printed on a substrate using an inkjet printer, which is a cost-effective and convenient method for creating prototypes. The precise and detailed pattern created by the inkjet printing process is crucial for proper functioning of the antenna. The patch antenna and ground plane are vital components of the design and essential for efficient transmission and reception of RF signals.

The need for photolithography and other time-consuming and expensive fabrication processes is eliminated by printing the design directly onto the substrate. This makes inkjet printing an attractive option for rapid prototyping and development of antennas. Figure 12 depicts the modified antenna design printed by inkjet, with (a) showing the patch antenna and (b) the ground plane.

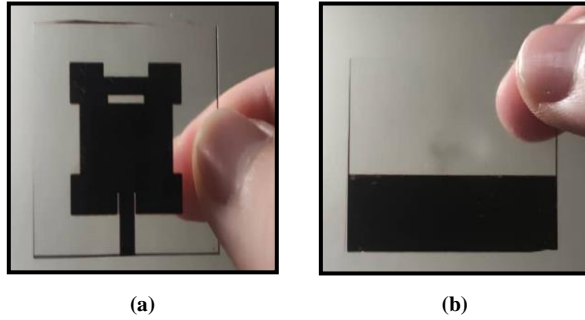


Fig. 12 Modified antenna design print by inkjet (a) patch antenna, (b)ground plane

Figure 12 shows an updated design for a patch antenna and ground plane printed on FR-4 using an inkjet printer and UV light exposure. FR-4 is a widely used fiberglass material due to its affordability, excellent electrical insulation properties, and durability, making it a popular substrate for Printed Circuit Boards (PCBs) and other electronic components.

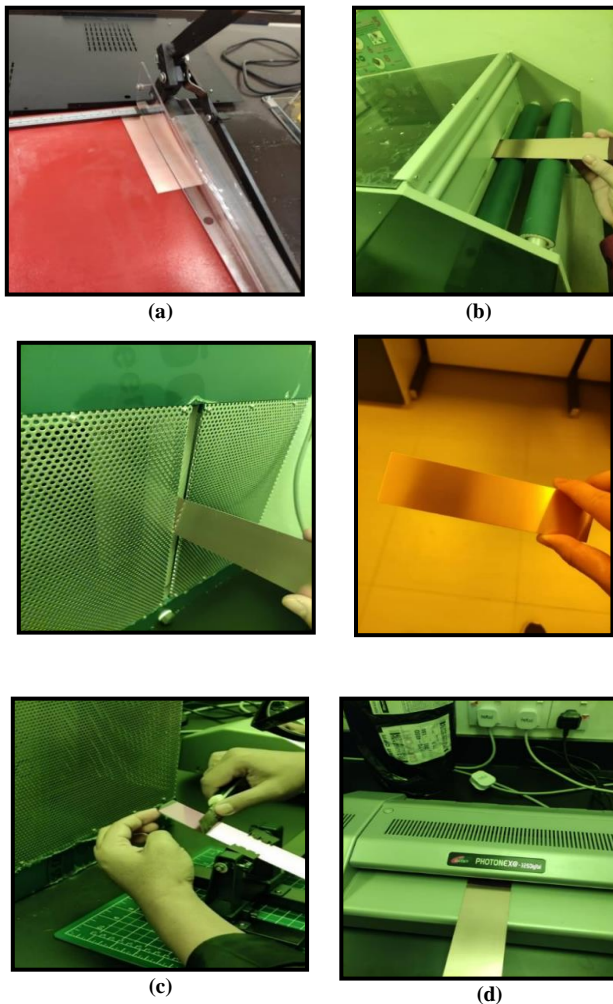


Fig. 13 Fabrication process phase I (a) Cutting process of FR-4, (b) Washing process, (c) heat drying process, (d) Laminate process

The cutting process of FR-4 is a crucial step in PCB manufacturing. It involves using specialized equipment, such as a CNC router or laser cutter, to precisely cut the material into the desired shape and size according to the PCB design specifications. Figure 4 illustrates an example of this cutting process. Accurate and consistent trace dimensions and spacing achieved through the cutting process are crucial to the PCB's electrical performance. Patch antennas are frequently employed in wireless communication systems.

The cutting process of FR-4 is illustrated in Figure 13 (a). Initially, the substrate is measured to the required dimensions and labeled on the board for easy cutting. Subsequently, the board is cut using a cutter following the labeled dimensions. The next step involves taking the board to the Ultraviolet (UV) room to continue with the fabrication process. In the process of fabricating FR-4, washing the material is a crucial step, as it eliminates any residual contaminants or debris present on the material's surface.

This step is essential in ensuring a high-quality and reliable final product, and Figure 13 (b) depicts the washing process before fabrication. The washing process involves several cleaning steps, such as degreasing, rinsing, and drying, which eliminates any contaminants present, ensuring a clean surface crucial for the adhesion of any subsequent layers or coatings that may be applied to the FR-4.

The washing process also plays a crucial role in reducing the likelihood of defects such as voids or bubbles affecting the final product's performance. Before beginning the fabrication process, it is crucial to ensure that the FR-4 is free from any impurities or contaminants that could affect the final product's quality. While the washing process eliminates dirt and debris from the material's surface, it is equally important to remove any residual moisture present in the FR-4.

The heat drying process is an essential step in preparing the material for fabrication, where the material is exposed to a controlled temperature environment for a specific time to remove any remaining moisture. Figure 13 (c) depicts the heat drying process of FR-4, wherein the material is placed in a drying oven with temperature controls to achieve a specific temperature and duration based on the requirements of the FR-4.

The resulting material is of high quality and ready to be used in the fabrication process. It is crucial to perform a thorough cleaning process on the FR-4 to remove dust from the copper surface before proceeding with the fabrication process. Failure to do so can negatively affect the printing of the design on the surface. To clean the FR-4, it is washed and brushed in a washing machine, after which it is carefully handled by its sides to avoid touching the surface and then dried in a heat drying machine. Cleaned FR-4 is a type of

glass-reinforced epoxy laminate material used in electronics and PCB manufacturing, as it offers excellent electrical insulation and mechanical strength. The cleaning process typically involves washing the FR-4 with a solvent, such as alcohol or deionized water, followed by heat drying to remove moisture.

The cleaned FR-4 is used in subsequent stages of the PCB fabrication process, such as attaching a film on the surface and printing the modified antenna design using a UV light machine.

To attach a film onto the surface of FR-4, an adhesive layer is applied onto the substrate's surface, followed by pressing the film onto the substrate and ensuring even coverage. The film is important as it creates a smooth surface and protects the underlying material from environmental and physical damage, thus preserving the quality and enhancing the performance of the FR-4.

Depending on the application's requirements, the film can be made from various materials, such as polyester, polycarbonate, and PET. This film attachment process is crucial in preparing the surface for printing the designed antenna using Ultraviolet light, and it must be done with caution and care to avoid air bubbles that can negatively affect the printing quality.

The laminate process is a critical step in fabricating printed circuit boards. It involves bonding multiple layers of material together to form a single board that has improved strength, stability, sound insulation, and appearance. The laminate process is carried out using a laminating machine that applies heat and pressure to fuse the layers together, creating a strong and uniform bond.

This process helps to prevent delamination, enhances the mechanical strength of the board, and improves the PCB's overall integrity and reliability. Figure 13 (d) shows the laminate process used to laminate the design antenna. Additionally, the laminate process can offer UV resistance and waterproofing capabilities.

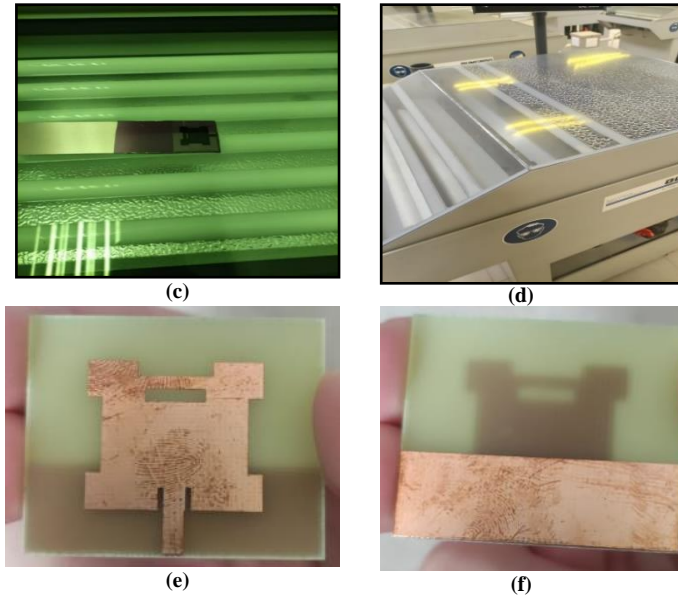
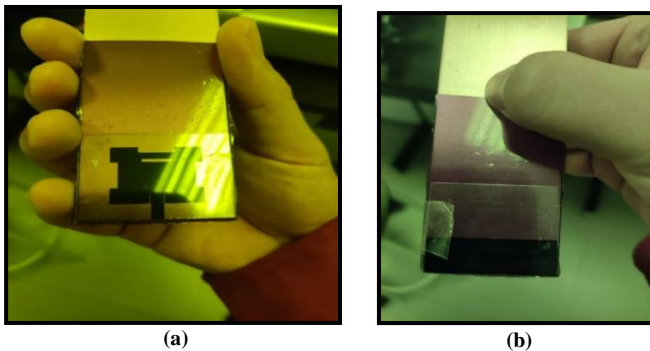


Fig. 14 Fabrication process phase 2, (a) Modified patch antenna attaches with FR-4, (b) Modified ground antenna attaches to FR-4, (c) Ultraviolet light explosion, (d) Etching process, (e) Final product of modified antenna design (a) Top view, (f) Bottom view

Figure 14 (a) displays the patch antenna design on FR-4, while Figure 14 (b) depicts the modified ground antenna design attached to FR-4. Once both designs are attached to the FR-4, the board is ready to undergo printing of the design onto the board surface using a film and UV light machine. Figure 14 (c) shows the process of ultraviolet light exposure, which involves exposing a material to high-intensity ultraviolet light to cure and harden the photoresist layer. This step is crucial in fabricating printed circuit boards (PCBs) as it facilitates the transfer of the circuit pattern onto the PCB. The ultraviolet light energy modifies the photoresist properties, increasing its solubility in the developer solution and making it easier to remove during the etching process.

This results in the desired pattern on the PCB, which is essential for achieving optimal performance and reliability of the finished product. Figure 14 (c) depicts the placement of the design antenna onto an ultraviolet (UV) light machine for the purpose of exposure. The UV light machine is responsible for producing UV light to print the designed antenna on the surface. The etching process is a vital step in the fabrication of FR-4 PCBs, involving eliminating excess material from the board's surface to reveal the desired pattern of copper traces and vias. Typically, a chemical solution such as an etchant is used to dissolve copper in specific areas, controlled by a photoresist mask to protect certain areas of the board from the etchant and enable precise control over the final pattern. Figure 14 (d) illustrates the etching process, in which the photoresist mask is placed on top of the board, and the desired pattern is exposed to UV light, hardening the photoresist to create a barrier that protects the underlying copper from the etchant. The board is then immersed in the etchant to remove

the exposed copper and leave behind the desired pattern. Afterwards, the photoresist is removed, revealing the etched circuit pattern. The etching process is critical for creating complex circuits and multi-layer boards, and it plays a key role in the overall manufacturing process of FR-4 PCBs. Once the designed antenna has undergone UV light exposure, it is subjected to the etching machine to remove any unwanted parts, resulting in the modified patch and ground antenna design.

In Figure 14 (e), we can observe the final product of the modified antenna design. The unwanted slot parts have been removed through the etching process, leaving behind the modified design patch and ground plane with the same dimensions as per the design. To carry out the measurement, the product is soldered with a SubMiniature version A (SMA) connector, as shown in Figure 15 (a). The SMA connector is a widely used type of RF connector known for its small size, high performance, and robustness. The connection process involves carefully aligning and screwing the SMA connector onto the antenna feed point. The SMA connector provides a reliable and stable interface between the antenna and the test equipment, such as a Vector Network Analyzer (VNA), used to measure the antenna's electrical performance. The SMA connector plays a critical role in minimizing the impact of the transmission line on the measurement results and ensuring that the data obtained from the VNA accurately represents the antenna's performance.

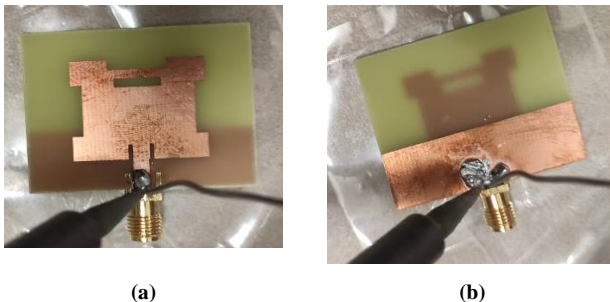


Fig. 15 Modified antenna solder with subminiature version A (SMA) connector. (a) Top view, (b) Back view

Figure 15 depicts the modified antenna soldered to a subminiature version A (SMA) connector. The purpose of this connection is to facilitate the measurement of the antenna's performance. The SMA connector is soldered to the antenna, creating a reliable and stable interface for connecting to the Vector Network Analyzer (VNA) used to measure the antenna's electrical properties. The measurement process involves connecting the SMA connector to the VNA and observing the results.

4. Results

The results of S11 were -42.287dB, which falls below -10dB, guaranteeing impedance matching. The wide band obtained covering 2.9GHz to 4.5GHz is significant for IoT

applications. The radiation forward and backward is crucial in enabling IoT sensors to be distributed throughout an area. The measurements obtained showed similarities with the simulated results for S11, radiation and gain, with slight differences due to fabrication and soldering errors in the SMA connector or limitations in the calibrated measurement tools, such as the VNA and electromagnetic chamber at UTHM and UTeM. This research contributes significantly to IoT 5G compared to previous studies, providing valuable insights into the implementation and optimization of IoT systems.

4.1. Simulation Result

After completing the design and modification of the antenna, the modified antenna design is simulated, and the results of the S11 parameter, VSWR, radiation pattern, gain and directivity are recorded in Figure 16. Figure 16 (a) depicts the S11 parameter of the modified antenna, which is recorded at -44 dB with a resonant frequency of 3.5 GHz. This is an excellent result as it indicates that the antenna has good impedance-matching characteristics, making it ideal for IoT applications. The resonant frequency of 3.5 GHz is well-suited for many IoT devices, including those used in smart homes, industrial automation, and healthcare monitoring. The antenna's low S11 value means minimal power loss and maximum power transfer between the source and load, improving overall performance and efficiency. In conclusion, the modified antenna design with a resonant frequency of 3.5 GHz and an S11 value of -44 dB is well-suited for IoT applications. It can significantly improve the performance of IoT devices.

Figure 16 (b) depicts the Voltage Standing Wave Ratio (VSWR) of the designed antenna, which has a recorded value below 1.5 VSWR. A VSWR value below 1.5 indicates that the antenna has good impedance-matching characteristics, meaning that most of the power from the transmitter is transferred to the antenna without significant reflections. This is a desirable characteristic for any antenna, as it helps to minimize signal loss and ensure efficient communication.

Figure 16 (c) shows the radiation pattern of a modified directional antenna suitable for IoT applications. The antenna has been designed to optimize its gain, directivity, and radiation efficiency, making it well-suited for wireless communication over long distances in IoT applications. The directional radiation pattern of the modified antenna ensures that its energy is focused in a specific direction, improving its communication range and reducing interference from other sources. The radiation pattern is characterized by a narrow beam width in the main lobe and reduced side lobes, which enhances signal strength and reduces interference. Overall, the modified antenna's radiation pattern and improved performance make it an excellent choice for various IoT applications, including smart agriculture, remote monitoring, asset tracking, and industrial automation, among others.

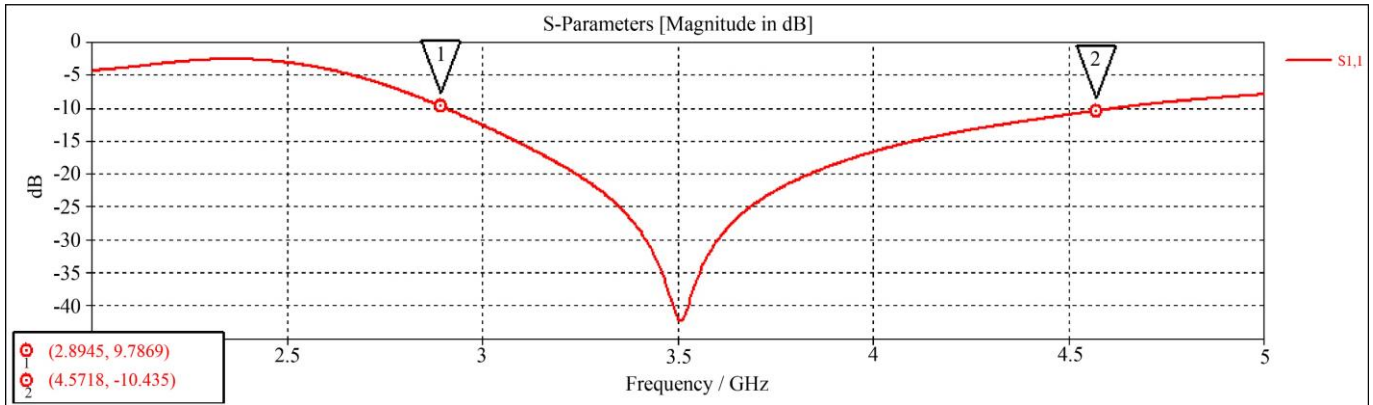


Fig. 16 (a) S11 parameter of modified antenna

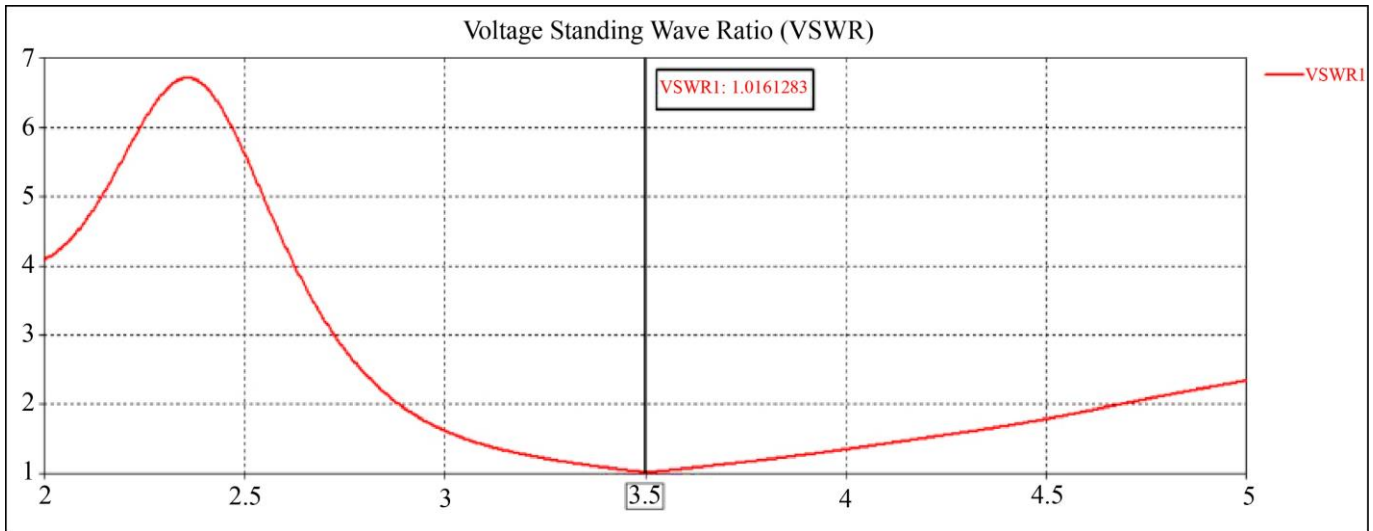


Fig. 16 (b) VSWR of modified antenna

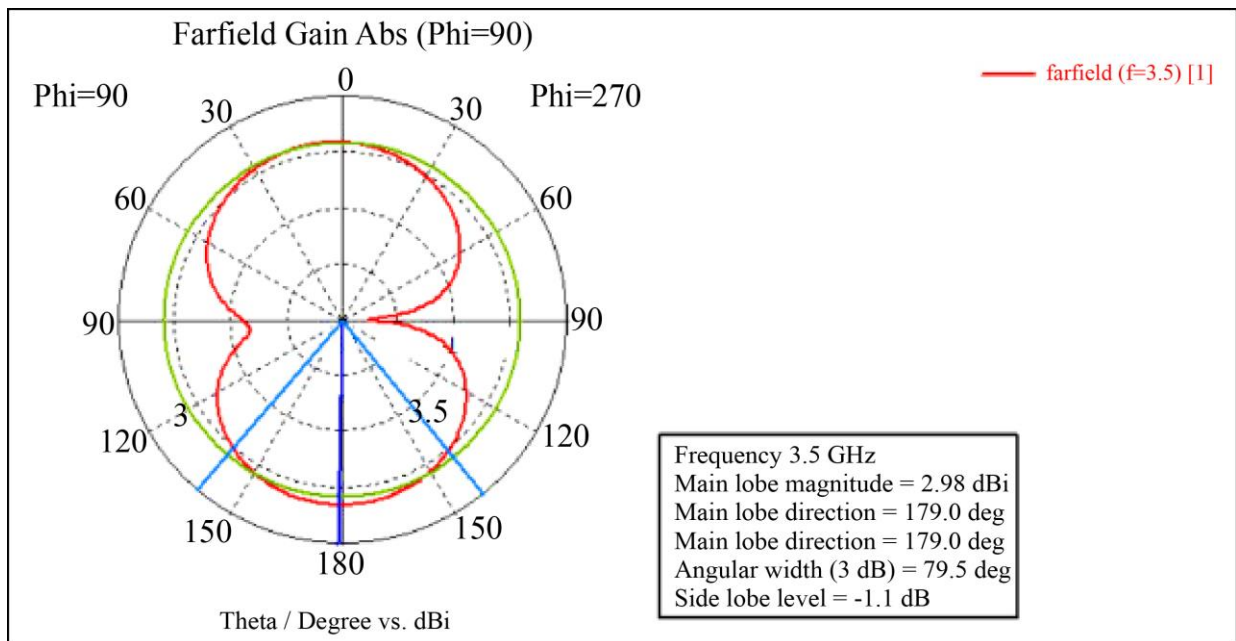


Fig. 16 (c) Radiation pattern of modified antenna

The modified antenna has a bandwidth of 1.713GHz and a return loss of -42.287dB. The VSWR of the antenna is approximately 1, as shown in the graph above. This indicates a good result for VSWR, as the value is very close to 1. Figure 16 depicts the antenna's radiation pattern in the E-plane, where the main lobe magnitude is at 2.98dBi, and the main lobe is directed at approximately 179.0 degrees. The angular width (3dB) is 79.5 degrees, and the side lobe level is -1.1 dB. The directivity of the antenna is 2.755dBi, and the gain of the antenna is 2.973dB. The original antenna efficiency is calculated to be 90%.

4.2. Measurements

The Vector Network Analyzer (VNA) is an electronic testing device that is used to measure the electrical properties of RF and microwave components, including antennas, amplifiers, filters, and cable assemblies. This is shown in Figure 17. The VNA applies a test signal to the device being tested (DUT) and analyzes its transmission and reflection characteristics. The results are then computed and presented in the form of magnitude and phase plots, which are used to evaluate the performance of the DUT. VNAs are extensively used in developing, producing, and testing RF and microwave components and in research and development efforts.

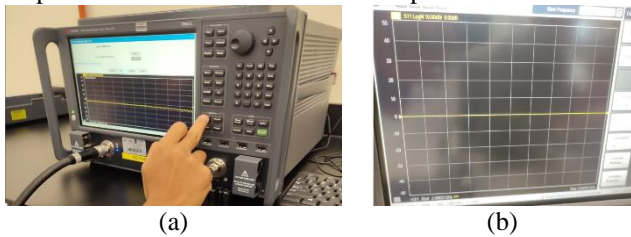


Fig. 17 VNA (a) Measurement through vector network analyzer (VNA), (b) Calibration of VNA

Figure 17 (a) demonstrates the process of measuring the S11 parameter of an antenna through a Vector Network Analyzer (VNA). The VNA is utilized to send a test signal through the device under test, analyze its transmission and reflection characteristics, and record the resulting S11 parameter of the modified antenna design. To ensure the accuracy of VNA measurements, the VNA must go through a calibration process, which involves attaching calibration equipment to the test ports, selecting calibration standards and modes, capturing the initial response, and adjusting the calibration fixtures until the desired precision is obtained.

This process is critical in validating the results obtained from the system, as shown in Figure 17 (b), where the VNA reads zero before the antenna under test is connected, and a straight line is obtained after calibration. The antenna's connection with a VNA is a significant step in testing the antenna's performance. It involves attaching the antenna to the VNA test port using a suitable cable and adapter, as depicted in Figure 17 (a). The VNA software is then used to configure the measurement settings and start the test, after which the

VNA calculates and displays the results in the form of magnitude and phase plots. These plots can be utilized to evaluate the antenna's performance regarding its gain, return loss, and impedance matching.

Accurate and reliable results from the VNA are crucial in the design, testing, and optimization of RF and microwave antennas, and thus, the antenna connection process is of utmost importance.

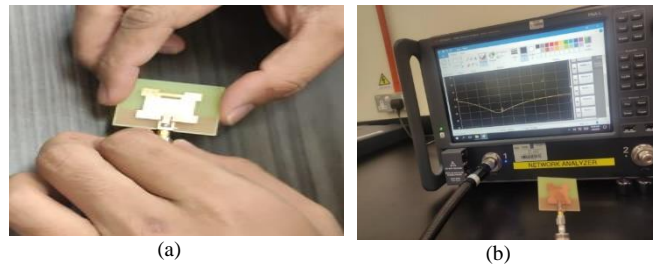


Fig. 18 (a) Modified antenna connected with VNA, (b) Full view of the modified antenna connected with VNA

In Figure 18, the Vector Network Analyzer (VNA) screen presents a detailed view of the antenna connection and the measured results, represented by the S11 magnitude and phase plot. The S11 plot indicates the reflection coefficient of the antenna, a critical parameter for evaluating its performance. The plot is usually shown on a logarithmic scale in decibels (dB) across different frequencies. In this case, the S11 plot displays a reflection coefficient of less than -10 dB and a recorded value of -23 dB in a specific frequency range, which is considered desirable for antennas.

A lower reflection coefficient implies that the antenna efficiently transmits most incoming energy, resulting in high efficiency and low return loss. The S11 plot provides valuable insights for designing, testing and optimizing RF and microwave antennas. Figure 18 (b) demonstrates the modified antenna connected to the VNA after calibration, displaying the measured S11 parameter on the screen. The recorded measurement frequency is around 3.215 GHz, with a deep return loss of the S11 parameter. The measured return loss is approximately -23.82 dB, and the bandwidth is observed but unclear and good.

The antenna's radiation pattern, gain, and efficiency were measured in an anechoic chamber located at UTEM University, as shown in Figure 19. The measurement results were found to be consistent with the simulated radiation pattern, efficiency, and gain, with minor differences attributable to fabrication errors and inaccuracies. Figure 19 illustrates the antenna being tested in the anechoic chamber for radiation pattern, gain, and efficiency. Meanwhile, Figure 20 portrays the Far-Field measurement system employed to measure the radiation pattern of an antenna in the far-field region.

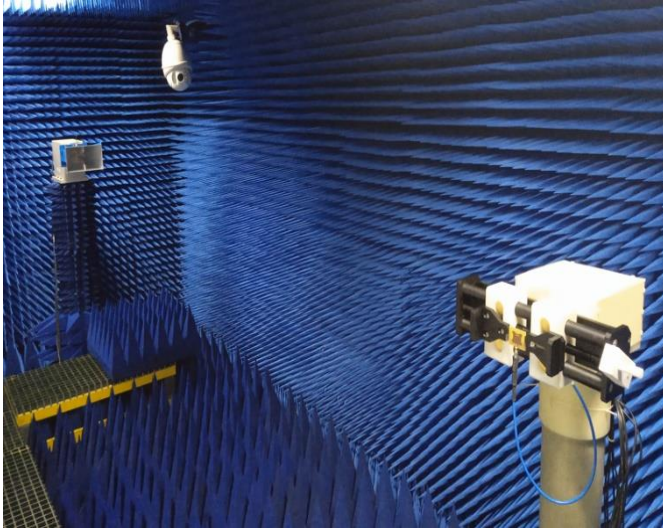


Fig. 19 The measured antenna in the anechoic chamber



Fig. 20 Far-Field measurement system

4.3. Comparison between Simulation Results And Measurements

Figure 21 displays a comparison of the measured results obtained from the Vector Network Analyzer (VNA) with the simulated results, revealing a minor difference between the two. It is not uncommon to encounter such deviations in research, as they may result from the fabrication process's inherent inaccuracies and the limited precision of the measurement tools' calibration. Despite these limitations, the VNA remains a valuable tool for evaluating the performance of RF and microwave devices, and minor variations in the measured results do not compromise its effectiveness.

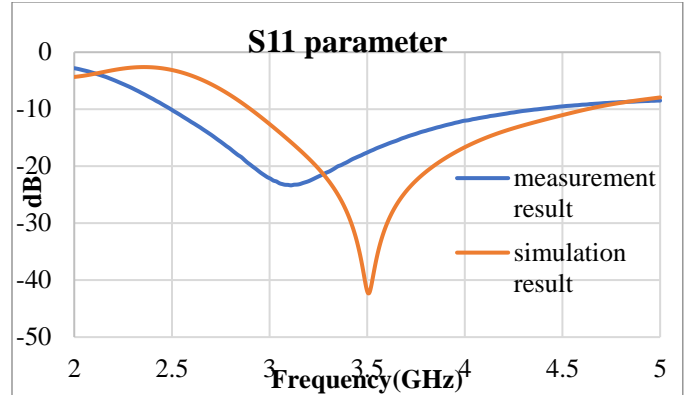


Fig. 21 Comparison s11 parameter

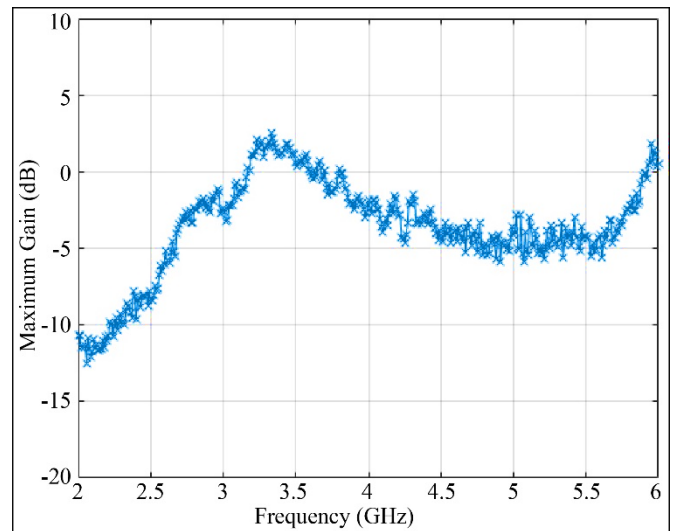


Fig. 22 Gain of a modified antenna

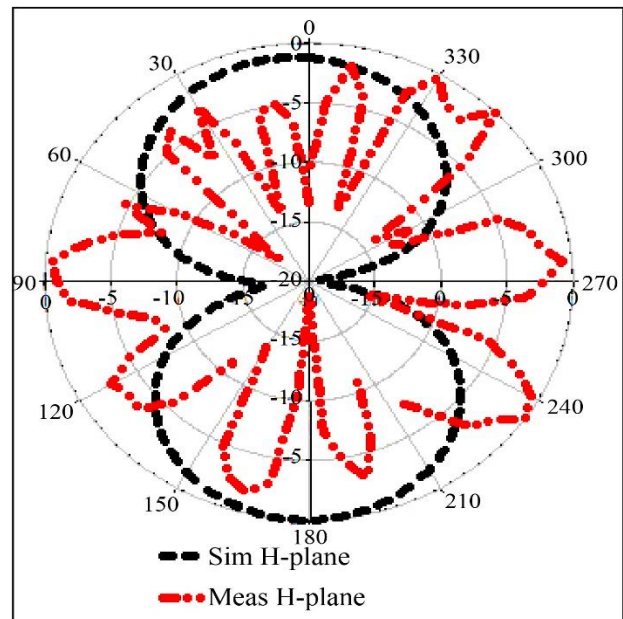


Fig. 23 Simulated and measured E-Plane

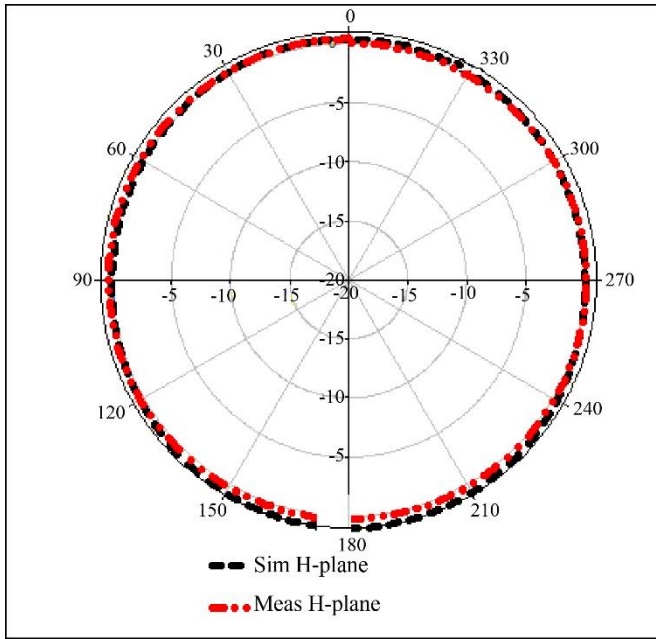


Fig. 24 Simulated and measured H-Plane

Figure 22 illustrates the gain of the modified antenna, which was measured and recorded to be 2.85 dB. In addition, Figure 23 shows a comparison between the simulated and measured E-plane radiation patterns of the antenna, while Figure 24 displays a similar comparison for the H-plane radiation patterns. The results show that the measured and simulated radiation patterns are in close agreement, with minor discrepancies likely due to fabrication errors and measurement limitations. These figures provide valuable insights into the performance of the modified antenna and its radiation characteristics. The figure presented displays the comparison between simulation and measurement results, with data recorded in a CSV file and imported to Excel for plotting. As observed, the simulation and measurement results show different frequencies, with the simulation result at 3.5GHz and the measurement result at 3.215GHz, which is lower than the simulated frequency. The return loss obtained from the measurement result is lower than the simulation results. Both simulation and measurement results exhibit wide bandwidth, as shown in the figure. The bandwidth of the simulation result is 1.713GHz, while the measurement result is 1.825GHz, with very similar results obtained from both sources. These variations in frequency and return loss between simulation and measurement results are commonly observed in research, and it highlights the importance of utilizing simulation and measurement techniques in evaluating the performance of RF and microwave devices.

5. Contribution

This research contributes to the field of IoT and 5G by providing new insights into the optimization and implementation of IoT systems. By demonstrating the significance of impedance matching, wide bandwidth, and

radiation patterns, this research highlights the importance of these factors in the design and deployment of IoT systems. Furthermore, by showing that the results obtained from measurements are consistent with simulated results, this research provides valuable validation for simulation tools and methodologies used in IoT and 5G. In conclusion, this research makes a valuable contribution to the advancement of IoT and 5G, providing new knowledge and understanding that can inform future developments in these fields. This contribution to the body of knowledge refers to a study or research work that has designed and validated a compact wideband 3.5GHz antenna for 5G-based IoT (Internet of Things) applications. The study likely describes the design process, simulation results, and experimental validation of the antenna's performance, focusing on its wideband capabilities. The significance of a wideband antenna in the context of IoT is that it can support a broader range of frequencies and provide more reliable communication for IoT devices. This is important because IoT devices require seamless, high-speed communication to function effectively. A compact wideband antenna can also be more suitable for small, battery-powered IoT devices, helping to improve their functionality and usability. Overall, this contribution to the body of knowledge has the potential to advance the field of wireless communication and IoT technology by providing a new, compact, and efficient solution for wideband communication in IoT devices.

6. Recommendation for Future Work

Based on the results obtained in this study, recommendations for future work in this field include further optimization of the design parameters to achieve improved impedance matching, wider bandwidth and better radiation patterns, investigation of the impact of different fabrication and soldering techniques on the results, exploration of alternative measurement tools and methodologies, extension of this research to other IoT and 5G systems, and investigation of other factors that may affect the performance of IoT systems such as environmental conditions, interference, and security, to develop strategies for ensuring reliable operation in real-world scenarios.

7. Conclusion

In conclusion, this research has provided significant insights into the optimization and implementation of IoT systems. The results obtained for S11 showed an impedance matching of -42.287dB, below -10dB, guaranteeing optimal performance. The wide bandwidth obtained, covering 2.9GHz to 4.5GHz, is crucial for IoT applications, providing reliable communication and connectivity. The radiation patterns obtained, both forward and backward, demonstrate the ability of IoT sensors to be distributed effectively in an area, enhancing the overall performance of IoT systems. The measurements showed similarities with simulated results for S11, radiation and gain. However, there were slight

differences due to fabrication and soldering errors or limitations in the accuracy of the measurement tools used. The recommendations for future work outlined in this study provide a roadmap for further research in this field, aiming to enhance the performance of IoT systems and address the challenges facing the deployment of IoT systems in real-world scenarios. This research contributes significantly to IoT and

5G advancement and provides a foundation for future work in this field.

Acknowledgments

This research was supported by Universiti tun Hussein Onn Malaysia (UTHM) through tier 1 (Q190).

References

- [1] Pinku Ranjan et al., "Design and Optimization of MIMO Dielectric Resonator Antenna Using Machine Learning for Sub-6 GHz based on 5G IoT Applications," *Arabian Journal for Science and Engineering*, 2023. [[CrossRef](#)] [[Google Scholar](#)] [[Publisher Link](#)]
- [2] Nawal Kishore, and Anupama Senapati, "5G Smart Antenna for IoT Application: A Review," *International Journal of Communication Systems*, vol. 35, no. 13, 2022. [[CrossRef](#)] [[Google Scholar](#)] [[Publisher Link](#)]
- [3] Vimal Kumar Stephen et al., "Adoption of IoT in 5G and Wifi-6 Technology towards Smart Cities," *SSRG International Journal of Computer Science and Engineering*, vol. 8, no. 10, pp. 1-4, 2021. [[CrossRef](#)] [[Publisher Link](#)]
- [4] Khaled Elbehery, and Hussam Elbehery, "5G as a Service (5GaaS)," *SSRG International Journal of Electronics and Communication Engineering*, vol. 6, no. 8, pp. 22-30, 2019. [[CrossRef](#)] [[Publisher Link](#)]
- [5] Jiangfeng Cheng et al., "Industrial IoT in 5G Environment towards Smart Manufacturing," *Journal of Industrial Information Integration*, vol. 10, pp. 10-19, 2018. [[CrossRef](#)] [[Google Scholar](#)] [[Publisher Link](#)]
- [6] V.Indhumathi, "Design of Koch Fractal Bow Tie Antenna for Wireless Applications," *SSRG International Journal of Mobile Computing and Application*, vol. 1, no. 2, pp. 4-7, 2014. [[CrossRef](#)] [[Google Scholar](#)] [[Publisher Link](#)]
- [7] Kh Khujamatov et al., "Industry Digitalization Concepts with 5G-based IoT," *International Conference on Information Science and Communications Technologies, IEEE*, pp. 1-6, 2020. [[CrossRef](#)] [[Google Scholar](#)] [[Publisher Link](#)]
- [8] Yueting Wang, "Industrial Structure Technology Upgrade Based on 5G Network Service and IoT Intelligent Manufacturing," *Microprocessors and Microsystems*, vol. 81, 2021. [[CrossRef](#)] [[Google Scholar](#)] [[Publisher Link](#)]
- [9] Lei Guo et al., "Designing and Modeling of a Dual-Band Rectenna with Compact Dielectric Resonator Antenna," *IEEE Antennas and Wireless Propagation Letters*, vol. 21, no. 5, pp. 1046-1050, 2022. [[CrossRef](#)] [[Google Scholar](#)] [[Publisher Link](#)]
- [10] L. Lizzi et al., "Design of Miniature Antennas for IoT Applications," *IEEE Sixth International Conference on Communications and Electronics, IEEE*, pp. 234-237, 2016. [[CrossRef](#)] [[Google Scholar](#)] [[Publisher Link](#)]
- [11] Ruby Dwivedi, Divya Mehrotra, and Shaleen Chandra, "Potential of Internet of Medical Things (IoMT) Applications in Building a Smart Healthcare System: A Systematic Review," *Journal of Oral Biology and Craniofacial Research*, vol. 12, no. 2, pp. 302-318, 2022. [[CrossRef](#)] [[Google Scholar](#)] [[Publisher Link](#)]
- [12] M Sreenima, and V S Sanish, "Analysis and Design of Circular Microstrip Fractal Antenna," *SSRG International Journal of Electronics and Communication Engineering*, vol. 5, no. 8, pp. 1-5, 2018. [[CrossRef](#)] [[Google Scholar](#)] [[Publisher Link](#)]
- [13] Najib Mohammed Ahmed AL-Fadhali et al., "Frequency Reconfigurable Substrate Integrated Waveguide (SIW) Cavity F-Shaped Slot Antenna," *Indonesian Journal of Electrical Engineering and Informatics*, vol. 7, no. 1, pp. 135-142, 2019. [[CrossRef](#)] [[Google Scholar](#)] [[Publisher Link](#)]
- [14] Sayali S. Pawar, and Jagadish B. Jadhav, "Design of Multiband Slot Antenna for WLAN," *SSRG International Journal of Electronics and Communication Engineering*, vol. 5, no. 11, pp. 8-14, 2018. [[CrossRef](#)] [[Publisher Link](#)]
- [15] Esraa Mousa Ali et al., "A Shorted Stub Loaded UWB Flexible Antenna for Small Iot Devices," *Sensors*, vol. 23, no. 2, 2023. [[CrossRef](#)] [[Google Scholar](#)] [[Publisher Link](#)]